Gas-Induced Solitons

L. Bergé and A. Couairon

Commissariat à l'Énergie Atomique, Département de Physique Théorique et Appliquée, B.P. 12, 91680 Bruyères-le-Châtel, France

(Received 10 July 2000)

The self-guiding of femtosecond laser pulses in air is investigated. For powers close to the threshold for self-focusing, we show that the balance between the nonlinear focusing of the beam and its defocusing by multiphoton sources produces a new kind of solitonlike structure. Over considerably long distances, the radial profile of the pulse relaxes to a steady-state shape, whereas its temporal profile shrinks along propagation. The influence of the normal group-velocity dispersion is finally discussed.

DOI: 10.1103/PhysRevLett.86.1003 PACS numbers: 42.65.Tg, 05.45.Yv, 42.65.Jx, 42.68.Ay

Femtosecond laser beams with high peak power have experimentally been observed to propagate by self-channeling over several Rayleigh lengths in the atmosphere [1–6]. Since the pioneering work by Braun *et al.* [1], numerous investigations have been devoted to model this spectacular propagation [6–10], which mainly proceeds from the balance between the Kerr response of air, that overcomes diffraction and focuses the pulse when its input power exceeds the self-focusing threshold, $P_{\rm cr}$, and the defocusing action of self-induced ionization. Among these theoretical attempts, two main scenarios have emerged to support the experimental features. First, the "moving-focus" model was proposed [6] as an intuitive approach of the spatiotemporal dynamics of ultrashort pulses in air. According to this model, the pulse is stacked into transverse slices in the time direction. The slices towards the center of the pulse contain powers exceeding $P_{\rm cr}$, whereas those on the wings are below critical. Consequently, the center of the pulse undergoes a collapse that develops all the faster as the power is high [11]. The end result is that, instead of being a focus point, the nonlinear focal region is spread out along the propagation axis. The longest slice then corresponds to peak power exactly equal to critical, for which the right balance between diffraction and nonlinear focusing is realized. This explanation succeeds in describing the initial optical phase in the formation of light channels. However, it cannot account for plasma generation and subsequent self-guiding of light that persists well beyond the linear focus of convergent beams [3]. On the basis of numerical simulations [8], a second scenario was recently stressed instead, following which the formation of light guides is dynamic and highly sensitive to the electron plasma created by ionization. First, the self-focusing beam generates a narrow plasma which strongly defocuses the trailing part of the pulse and produces one leading peak. Once the intensity decreases enough, plasma generation turns off. The back of the pulse can then focus again, which finally creates a two-spiked structure in the wave temporal profile. This sequence of events can repeat many times in principle and light guiding results from the so-called "dynamic spatial replenishment of light" [8]. This scenario was observed for peak powers above $5P_{\rm cr}$ and most of its characteristic stages were later confirmed at higher power levels [10].

From these different analyses, it appears that the optically induced ionization not only arrests the collapse and possibly "stabilizes" the beam over long distances, but also distorts the temporal shape of the pulse. We can thus wonder whether there exists a fundamental structure, which could efficiently sustain the beam by relying on the saturating effects carried out by the electron plasma, while accounting for such temporal distortions. In this paper, we address the question of determining the basic structure that a pulse may keep along propagation in the atmosphere. We show that a pulse envelope with power close to critical and coupled with an electron plasma created by multiphoton ionization (MPI) can indeed evolve to a new robust waveform. In the absence of group-velocity dispersion (GVD), this wave packet exhibits a temporal profile having only a leading peak that shrinks on the time axis. In the diffraction plane, the pulse converges to a steady-state object and behaves like a spatial soliton. As a result, a new kind of light guide arises, stable transversally while shrinking temporally, and capable of persisting over considerable distances. The variations in time caused by GVD and expected to stop the temporal compression of this elementary structure are finally studied.

Our model consists of an extended nonlinear Schrödinger (NLS) equation governing the slowly varying envelope of the laser electric field, $\mathcal{E}(\vec{r},t,z)$, coupled with the density, $\rho(\vec{r},t,z)$, of electron plasma resulting from ionization. Expressed in the reference frame moving at the group velocity, i.e., the variable t refers to the retarded time variable $t - z/v_g$ with $v_g \equiv [\partial k/\partial\omega|_{\omega_0}]^{-1}$, the propagation equation for $\mathcal{E}$ reads

$$2ik_0\partial_z\mathcal{E} + \Delta_\perp\mathcal{E} + 2k_0^2 n_2|\mathcal{E}|^2\mathcal{E} - k_0^2\frac{\rho}{\rho_c}\mathcal{E} = 0. \quad (1)$$

Here z is the propagation length, the Laplacian models the wave diffraction in the transverse plane, k_0 and ω_0 are the wave number and frequency of the carrier wave, n_2 denotes the nonlinear refraction index in the Kerr response

of air entering $P_{\rm cr} \simeq \lambda_0^2/2\pi n_2$, and ρ_c is the plasma critical density. Following Keldysh's theory [12], we assume that MPI dominates for peak intensities less than 10^{14} W/cm^2 and, therefore, an atom with ionization potential U_i is ionized by the absorption of K photons with energy $\hbar\omega_0$ [$K = \mathrm{mod}(U_i/\hbar\omega_0) + 1$]. The electron density thus obeys

$$\partial_t \rho = \sigma |\mathcal{E}|^{2K} (\rho_{\rm at} - \rho), \qquad (2)$$

where the coefficient σ is related to the cross section for inverse bremsstrahlung and ρ never exceeds a few percent of the initial atom density $\rho_{\rm at} = 2.7 \times 10^{19}$ cm$^{-3} \ll \rho_c = 1.8 \times 10^{21}$ cm^{-3}. We first disregard the GVD of the beam, as in self-focusing regimes the dominant effect altering the temporal profile of pulses with about 200 fs duration is mainly MPI [10]. In addition, because energy losses are of little influence in the pulse propagation, we also neglect plasma and multiphoton absorptions. For simplicity, the Kerr response of air is considered only as instantaneous and delayed components [13] are omitted. In typical experiments, one has at atmospheric pressure $n_2 = 3.2 \times 10^{-19}$ cm^2/W, $K = 10$ with $U_i = 14.6$ eV at the laser wavelength $\lambda_0 = 800$ nm, $\sigma \simeq 10^{-128}$ W^{-10} cm^{20} s^{-1}, and the critical self-focusing power is $P_{\rm cr} \simeq 3.2$ GW. The input pulse is a collimated Gaussian beam, $\mathcal{E}(r,t,0) = \sqrt{2P_{\rm in}/\pi w_0^2}\, e^{-r^2/w_0^2 - t^2/t_p^2}$, with temporal half-width $t_p = 170$ fs, waist $w_0 = 1$ mm, and Rayleigh length $z_0 = \pi w_0^2/\lambda_0 \simeq 4$ m. $P_{\rm in}$ is the peak input power entering the transverse power of the beam, $P_\perp(t) = \int |\mathcal{E}|^2 \, d\vec{r}$, which is preserved along z at each given instant.

We have numerically integrated the model equations (1) and (2) for the input power $P_{\rm in} = 1.25 P_{\rm cr}$ and initial density $\rho_0 = 0$. The numerical scheme for solving (1) was elaborated on a Crank-Nicholson implicit method applied to each transverse slice along time. The density equation (2) was resolved at each position (r,z) by an adaptive time-step Runge-Kutta method, ensuring a relative error smaller than 10^{-3}. Only steps coinciding with the grid points used to integrate Eq. (1) were retained in the coupling. By varying the resolution, the simulations revealed identical features, up to small-amplitude oscillations that we ignore. The results are plotted in Fig. 1. Figure 1(a) shows the maximum-in-time intensity of the pulse centered at $r = 0$ along the z axis. It displays the formation of a plateau, which remains clamped to around the same maximum value beyond $z_0 = 4$ m. A similar behavior was earlier discovered in [1], which was interpreted in terms of self-channeling issued from the balance between Kerr focusing and a static decrease of the optical index caused by the electron plasma. Nonetheless, the pulse dynamics detailed below appears to be more complex. Indeed, Fig. 1(b) shows that the on-axis fluence distribution $F(z) = \int |\mathcal{E}(t)|^2 \, dt$ does not remain fixed, but instead increases up to a nonlinear focus at $z \sim 5$ m, then decreases to a value comparable with the incident fluence at $z \sim 10$ m. The pulse radius measured as the width

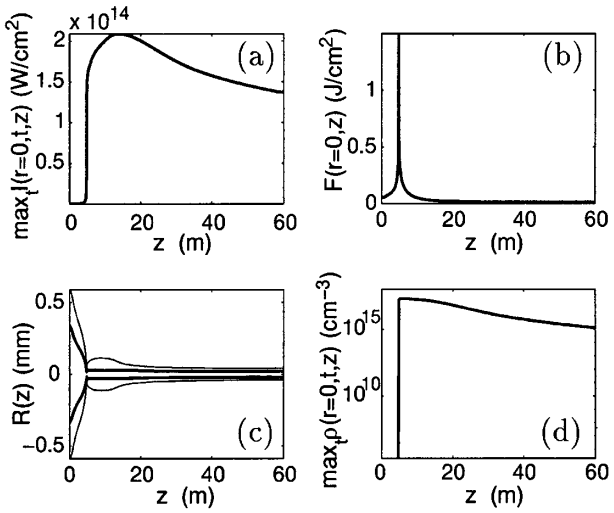

FIG. 1. Dynamics of Gaussian beam with $P_{\rm in} = 1.25 P_{\rm cr}$: (a) Maximum-in-time intensity, (b) fluence, (c) beam radius, and (d) maximum-in-time density, all measured on axis $r = 0$.

at half-maximum of the fluence distribution remains quite steady, as shown in Fig. 1(c). It becomes almost uniform at large z and emphasizes the formation of a long waveguide. Finally the maximum density profile is illustrated in Fig. 1(d), where the ionization front holds a nearly constant level over 8 m, then slowly decreases afterwards. As a result, the total propagation domain exceeds 60 m, i.e., more than 15 Rayleigh lengths.

Two stages can clearly be distinguished in the propagation. First, the optical Kerr effect focuses the pulse, until the beam intensity becomes sufficiently large to excite the electron density. Second, a light guide forms and propagates over long distances, by being coupled with a significant electron density level. During this stage the electron plasma defocuses the trail of the pulse and strongly shortens its leading edge around and beyond the nonlinear focus. At larger z, we can expect that the pulse may ultimately diffract as ρ decreases to zero. Figure 2 shows the stabilization of the radial distribution in the pulse intensity [Fig. 2(a)] and the distortions undergone by the temporal profile of the pulse at four different propagation distances [Figs. 2(b)–2(e)]. These results provide evidence that, after the nonlinear focus, the beam does relax to a transverse shape almost stabilized in the diffraction plane and thus exhibits a structure resembling a spatial soliton. Temporally, the pulse becomes localized at times close to $t \simeq -60$ fs. Compared with earlier propagation, we also observe that near this instant the deformations in the temporal profile are quasistationary, although the pulse still slowly moves back in time. On the whole, beyond the nonlinear focus, the leading part of the pulse becomes very spiky with limited amplitude and undergoes sharp temporal gradients. In contrast, the trailing part is totally depleted by the electron plasma. This spiky structure persists in the vicinity of the transverse slice of time that contains exactly

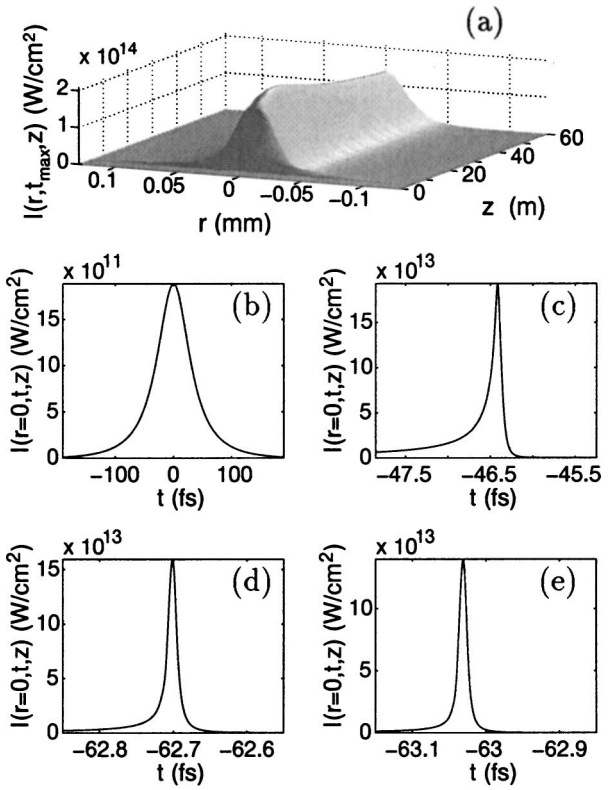

FIG. 2. (a) Radial beam intensity profile $I \equiv |\mathcal{E}|^2$ vs (r, z) at times $t_{\max}$, for which the pulse amplitude is maximum. Temporal distributions $|\mathcal{E}|^2$ vs t at the propagation distances (b) $z = 4$ m, (c) $z = 8$ m, (d) $z = 40$ m, and (e) $z = 60$ m.

the critical power for self-focusing at $z = 0$, i.e., $t^* \equiv -(\ln\sqrt{P_{\rm in}/P_{\rm cr}})^{1/2} t_p \simeq -57$ fs.

To justify these observations, we rescale Eqs. (1) and (2) with the substitutions $z \to 4z_0 z$, $r \to w_0 r$, $t \to t_p t$, $\rho \to \rho_{\rm at}\rho$, $\mathcal{E} \to \sqrt{2P_{\rm in}/\pi w_0^2}\,\mathcal{E}$, and introduce the constants $a = 8P_{\rm in}/P_{\rm cr}$, $b = k_0^2 w_0^2 \rho_{\rm at}/\rho_c$, and $c = \sigma t_p (2P_{\rm cr}/\pi w_0^2)^K$ for notational convenience. Expressed in these dimensionless units, localized wave fields $\mathcal{E}$ have a mean-square radius, $\langle r^2\rangle \equiv P_\perp^{-1} \int r^2 |\mathcal{E}|^2 \, d\vec{r}$, satisfying the identity [10]

$$\partial_z^2 \langle r^2\rangle = \frac{4}{P_\perp} \int \{2|\vec{\nabla}_\perp \mathcal{E}|^2 - a|\mathcal{E}|^4 - b|\mathcal{E}|^2 \vec{r}\cdot\vec{\nabla}_\perp \rho\}\, d\vec{r}\,. \quad (3)$$

For a density profile decreasing from $r = 0$, this equation indicates that at sufficient powers the self-focusing process described by the decrease of $\langle r^2\rangle$ is stopped as ρ strongly increases with $|\mathcal{E}|$. We then perform the self-similarlike transformation

$$\mathcal{E}(r,t,z) = \frac{\phi(\xi,t,\zeta)}{R(z,t)}\, e^{i\lambda\zeta + iR_z R\xi^2/4}, \quad (4)$$

where $\xi = r/R(z,t)$, $\zeta = \int_0^z du/R^2(u,t)$, and the parameter $\lambda > 0$ assures us that ϕ vanishes at infinity like a discrete NLS eigenmode. Here $R(z,t)$ denotes the average radius of the wave field varying both in time and along z. For self-focusing beams, we assume that ϕ behaves self-similarly with $\partial_\zeta \phi \to 0$ and is close to a real profile function. Under these assumptions, we plug (4) into Eq. (3) and obtain

$$\frac{V}{4} R^3 R_{zz} = X - \frac{aY}{2} - \frac{bR^2}{2} \int |\phi|^2 \vec{\xi}\cdot\vec{\nabla}_\xi \rho \, d\vec{\xi}\,, \quad (5)$$

where $\partial_t \rho = c(P_{\rm in}/P_{\rm cr})^K |\phi|^{2K}/R^{2K}$, $X = \int |\vec{\nabla}_\xi \phi|^2 \, d\vec{\xi}$, $Y = \int |\phi|^4 \, d\vec{\xi}$, $V = \int \xi^2 |\phi|^2 \, d\vec{\xi}$, and $\vec{\nabla}_\xi$ means differentiation with respect to ξ. Equation (5) shows that the pulse tends to collapse with $R \to 0$ and $R_{zz} < 0$, as long as $4P_{\rm in} Y/XP_{\rm cr} > 1$. However, collapse is arrested by MPI as the integal term of (5), scaling as R^{2-2K}, is negative. More precisely, since ϕ has a temporal component, the electron density ρ first defocuses the transverse slices of highest peak power and thus shortens the pulse duration, which thereby leads to $R_t/R < 0$.

We can then determine the conditions under which a self-guided beam may be realized with a radius reaching a steady-state value, $R_{zz} \to 0$. To this aim, we first multiply Eq. (1) by the complex conjugates of $\mathcal{E}$ and $t\partial_t \mathcal{E}$, and combine the real parts of the results that we integrate over space and in time between 0 and infinity. After inserting Eq. (4) where $\partial_\zeta \phi \to 0$ and canceling the z derivatives of $R(z,t)$, we find the relation

$$\int_0^{+\infty} \left\{ \frac{aY}{2} + t\left[\frac{bc}{R^{2K-2}} \left(\frac{P_{\rm in}}{P_{\rm cr}}\right)^K \times \int |\phi|^{2K+2} \, d\vec{\xi} - 4\lambda P_\perp \frac{R_t}{R} \right] \right\} \frac{dt}{R^2} = 0\,, \quad (6)$$

which shows that a steady-state light guide can exist at negative times only. Next, the time coordinate towards which the pulse converges is estimated by means of Eq. (5) in the framework of a variational approach, which is known to reproduce the qualitative behaviors of the beam [10]. Let us consider the trial function $\phi(\xi,t) = \sqrt{I(t)}\, e^{-\xi^2/2}$ with $I(t) = \frac{1}{2} e^{-2t^2}$ and $R(0,t) = 1/\sqrt{2}$ that fits the incident Gaussian pulse at $z = 0$. In the light of Fig. 2, we suppose that as $R_{zz} \to 0$ the variations in time of $R(z,t)$ are slow and negligible compared with the exponential decrease of $I(t)$, i.e., $R(z,t) \propto \sqrt{\langle r^2\rangle}$ is almost frozen in time with $R_t/R \ll I_t/I$. Equation (5) then provides the variational estimate

$$\int_{-\infty}^{t} e^{-2Kt'^2}\, dt' \simeq \frac{(P_{\rm in}/P_{\rm cr}) e^{-2t^2} - 1}{\beta (P_{\rm in}/P_{\rm cr})^K R^{2-2K}}\,, \quad (7)$$

with $\beta = Kbc/2^K(K+1)^2$. From Eqs. (6) and (7), steady-state solutions can exist only at times close to $t \simeq t^* \equiv -(\ln\sqrt{P_{\rm in}/P_{\rm cr}})^{1/2}$ in units t_p, which agrees with the numerical results. This estimate can be refined by choosing a trial function different from Gaussian, as, e.g., the NLS ground-state solution to $-\phi_0 + \Delta_\xi \phi_0 + \phi_0^3 = 0$ having the lowest power for collapse $\int \phi_0^2 \, d\vec{\xi} = 11.7$. This amounts to introducing

the ratio $4\pi/11.7$ in front of $P_{\rm in}/P_{\rm cr}$ [10], which provides the enhanced moment $t^* \simeq -65$ fs. This instant is in better agreement with Fig. 2(e), and it locates the slice containing exactly the minimum bound of power for self-focusing.

We observe that if the beam size reached a strictly constant-in-time equilibrium radius $R_{\rm eq}$ [$\partial_z R_{\rm eq} = \partial_t R_{\rm eq} = 0$], the above relations would characterize nonlinear ground states for Eq. (1), defined in the standard form $\mathcal{E}(r,t,z) = \phi(r,t)e^{i\lambda z}$, with ϕ decaying to zero at infinity. Therefore, although the temporal shape of the pulse can here slowly move under the limit $R_{zz} \to 0$, we term these new objects as "gas-induced solitons." Previous analytical investigations based on similar variational methods [7] already suggested the possibility of producing stable solitons, resulting from the nonlinear saturation of the Kerr response in the radial plane by MPI. However, the inner temporal dynamics of the beam was disregarded in Ref. [7], and these structures were believed to exist around the central slice $t = 0$.

Let us now discuss the influence of normal GVD, as the pulse becomes so shrunk in the time direction, that the NLS model (1) must include refinements from the basic paraxial description of the optical self-focusing. Among those, we select only GVD contributions, which become relevant as the pulse shape attains durations below 10 fs. GVD can formally be taken into account by adding $-k_0 k'' \partial_t^2 \mathcal{E}$ into Eq. (1). In the absence of MPI, this term arrests the collapse near the slice $t = 0$ of strongest power and splits the beam into two symmetric spikes [14]. In contrast, MPI tends to defocus the trailing pulse and forms a narrow leading spike only. Figure 3 shows the influence of GVD for different values of k'', at different propagation distances between one and two Rayleigh lengths. For a strong dispersion coefficient, $k'' = 2.0$ fs^2/cm, the beam splits and disperses before MPI becomes a key player. Conversely, at the lower value $k'' = 0.2$ fs^2/cm, which is commonly accepted by experimentalists for infrared pulses in air [15], MPI takes over GVD. So, even though GVD surely alters the full development of gas-induced solitons, the early stages in their formation can play an important role in the self-guiding of light, at least over the first Rayleigh lengths. In this regard, it is worth noticing that Fig. 1(c) shows the reduction of the beam diameter to around $1/20$ times its input value (2 mm). With an energy $E_{\rm in} = \int P_\perp(t)\,dt \simeq 0.85$ mJ, a filament of about 100 μm diameter then emerges. These data are in a remarkable agreement with the size (80–100 μm) and energy (0.7–1 mJ) measurements of filaments generically observed in experiments [1–3].

In conclusion, we have identified the nonlinear waveguide mode to which light waves coupled with a MPI source evolve when they propagate through the atmosphere. In particular, we have emphasized the peculiar nature of the temporal distribution of these new objects, termed as gas-induced solitons. Such structures exhibit

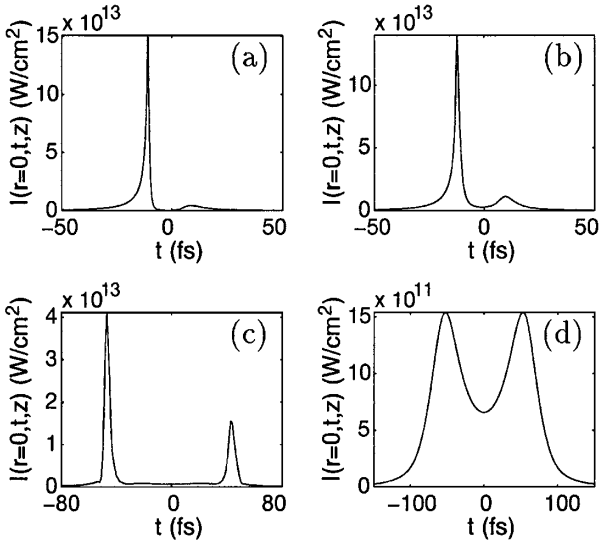

FIG. 3. Temporal intensity profiles at center $r = 0$ for propagation distances $\leq 2z_0$ and different GVD coefficients: (a) $k'' = 0$, $z = 5$ m, (b) $k'' = 0.2$ fs^2/cm, $z = 5.1$ m, (c) $k'' = 0.8$ fs^2/cm, $z = 6$ m, (d) $k'' = 2$ fs^2/cm, $z = 7$ m.

a single leading peak located at negative instants and a quasistable transverse distribution. Although self-compressing in time, they are capable of sustaining a long propagation covering here more than 60 m. Thus, multiphoton ionization provides a key mechanism that does not only regularize the collapse, but also makes self-guided pulses rather robust in gases. Further studies should concern the fate of these solitonlike waveguides in the presence of second-order temporal deviations from the time-envelope approximation [16] and of delayed Kerr components [13].

[1] A. Braun, G. Korn, X. Liu, D. Du, J. Squier, and G. Mourou, Opt. Lett. **20**, 73 (1995).
[2] E. T. J. Nibbering *et al.,* Opt. Lett. **21**, 62 (1996).
[3] H. R. Lange *et al.,* Opt. Lett. **23**, 120 (1998).
[4] B. La Fontaine *et al.,* Phys. Plasmas **6**, 1615 (1999).
[5] L. Wöste *et al.,* Laser Optoelektron. **29**, 51 (1997).
[6] A. Brodeur, C. Y. Chien, F. A. Ilkov, S. L. Chin, O. G. Kosareva, and V. P. Kandidov, Opt. Lett. **22**, 304 (1997); O. G. Kosareva, V. P. Kandidov, A. Brodeur, C. Y. Chien, and S. L. Chin, *ibid.* **22**, 1332 (1997).
[7] S. Henz and J. Herrmann, Phys. Rev. E **53**, 4092 (1996).
[8] M. Mlejnek, E. M. Wright, and J. V. Moloney, Opt. Lett. **23**, 382 (1998).
[9] A. Chiron *et al.,* Eur. Phys. J. D **6**, 383 (1999).
[10] L. Bergé and A. Couairon, Phys. Plasmas **7**, 210 (2000).
[11] J. H. Marburger, Prog. Quantum Electron. **4**, 35 (1975).
[12] L. V. Keldysh, Sov. Phys. JETP **20**, 1307 (1965).
[13] J. F. Ripoche *et al.,* Opt. Commun. **135**, 310 (1997).
[14] P. Chernev and V. Petrov, Opt. Lett. **17**, 172 (1992).
[15] C. Allen, *Astrophysical Quantities*, (University of London, London, 1964).
[16] A. L. Gaeta, Phys. Rev. Lett. **84**, 3582 (2000).